Provided for non-commercial research and education use.
Not for reproduction, distribution or commercial use.

This article appeared in a journal published by Elsevier. The attached copy is furnished to the author for internal non-commercial research and education use, including for instruction at the authors institution and sharing with colleagues.

Other uses, including reproduction and distribution, or selling or licensing copies, or posting to personal, institutional or third party websites are prohibited.

In most cases authors are permitted to post their version of the article (e.g. in Word or Tex form) to their personal website or institutional repository. Authors requiring further information regarding Elsevier's archiving and manuscript policies are encouraged to visit:

http://www.elsevier.com/copyright

Author's personal copy

Journal of Crystal Growth 311 (2008) 54–58

Contents lists available at ScienceDirect

Journal of Crystal Growth

journal homepage: www.elsevier.com/locate/jcrysgro

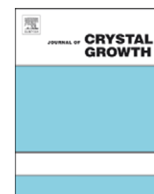

Large-grained oriented polycrystalline silicon thin films prepared by nickel-silicide-induced crystallization

J.A. Schmidt [a,b,*], N. Budini [a], P. Rinaldi [a], R.D. Arce [a,b], R.H. Buitrago [a,b]

[a] Instituto de Desarrollo Tecnológico para la Industria Química, UNL–CONICET, Güemes 3450, S3000GLN Santa Fe, Argentina
[b] Facultad de Ingeniería Química, UNL, Santiago del Estero 2829, S3000AOM Santa Fe, Argentina

ARTICLE INFO

Article history:
Received 29 July 2008
Received in revised form
3 October 2008
Accepted 12 October 2008
Communicated by D.W. Shaw
Available online 18 October 2008

PACS:
68.55.A–
81.10.Jt
68.55.–a

Keywords:
A1. Optical microscopy
A1. Recrystallization
A1. X-ray diffraction
A2. Seed crystals
B2. Semiconducting silicon
B3. Solar cells

ABSTRACT

Nickel-silicide-induced crystallization of hydrogenated amorphous silicon thin films has been investigated. Intrinsic and doped films were deposited on glass substrates by HF-PECVD, and Ni was dc sputtered on top. Nucleation and growth of grains were followed by optical microscopy, scanning electron microscopy (SEM), UV reflectance and X-ray diffraction. Homogeneous, large and oriented grains, with diameters over 25 μm, were obtained in intrinsic and lightly boron-doped films. Phosphorous-doped films presented a random needle-like growing mechanism, instead of the disk shape shown by the other samples. The effect of doping elements on the crystallization process is discussed.

© 2008 Elsevier B.V. All rights reserved.

1. Introduction

Polycrystalline silicon (poly-Si) in the form of thin films has attracted considerable attention as a base material to produce active-matrix liquid crystal displays, active-matrix organic light emitting diodes, and solar cells. Several methods of preparation have been developed, like the direct deposition of poly-Si in a CVD reactor at high temperatures, using hydrogen and chlorosilanes as reactant gases [1,2], or the indirect deposition through a crystallization process from amorphous silicon. The latter is the appropriate method when the substrate requires a low-temperature process, like the glass substrates to be used for solar cells [3–7] or for large-area imagers based on thin-film transistors [8].

Common methods of crystallizing amorphous silicon are solid phase crystallization (SPC), excimer laser annealing (ELA) and metal-induced crystallization (MIC) [9]. SPC, one of the first techniques explored to crystallize amorphous silicon [10], requires high temperatures and long annealing periods, which may cause cross-diffusion of dopants in the case of solar cells. ELA works at lower temperatures, but has the drawbacks of poor uniformity and high production costs [11,12]. The addition of some metals—like nickel—to amorphous silicon reduces the crystallization temperature in comparison to SPC, leading to a larger grain size with good uniformity. This MIC process overcomes the problems of ELA and SPC, and has been widely studied in connection to thin-film transistors (TFTs) for crystal displays [13]. When the crystal growth is in the lateral direction from a Ni electrode, the process is called metal-induced lateral crystallization (MILC) and it is possible to grow poly-Si at temperatures as low as 500 °C [3–6]. Most of the work done in the field of MIC and MILC for TFTs applications focused on thin samples, typically of <0.1 μm. In this work, we present results on samples of intermediate thickness, in the range of 0.3–0.5 μm.

Studies on the crystallization mechanisms and the dopant effects on MILC have been reported. Although there is an agreement regarding the formation of nickel disilicide ($NiSi_2$), and the diffusion of this species leaving behind crystalline silicon, the effect of the dopant atoms in a microstructural level is still

*Corresponding author at: Instituto de Desarrollo Tecnológico para la Industria Química, UNL-CONICET, Güemes 3450, S3000GLN Santa Fe, Argentina.
Tel.: +54 342 455 9175; fax: +54 342 455 0944.
E-mail address: jschmidt@intec.unl.edu.ar (J.A. Schmidt).

0022-0248/$ - see front matter © 2008 Elsevier B.V. All rights reserved.
doi:10.1016/j.jcrysgro.2008.10.027

Author's personal copy

unclear. Phosphorous is well known for its ability to getter transition metal elements, so it could trap a fraction of the $NiSi_2$, retarding the lateral crystallization or favoring the growth of crystal needles in some directions [6,14].

In this work, we present results of our current research on thin poly-Si layers grown by MIC for solar cell applications. Starting from an amorphous silicon layer, we look for a thermal process to induce a solid phase transformation, leading to a polycrystalline material with the largest possible grain size. Since we focus on solar cell applications, we studied the Ni-induced crystallization of the three individual layers that together form a cell, namely (i) the n^+ layer, strongly doped with P ($\sim 10^{19}$ at/cm^3), (ii) the p layer, slightly doped with B ($\sim 10^{16}$ at/cm^3), and (iii) the p^+ layer, strongly doped with B ($\sim 10^{19}$ at/cm^3). Different Ni concentrations and annealing temperatures have been studied, trying to establish the optimum thermal treatment.

2. Experimental details

Samples were prepared on Schott AF-37 glass in a capacitively coupled plasma enhanced chemical vapor deposition (PECVD) reactor. We used a relatively high frequency of 50 MHz and a power density of 120 mW/cm^2, the distance between electrodes being 1.1 cm. As reactant gases we used silane (SiH_4), phosphine (PH_3, for n-type doping) and diborane (B_2H_6, for p-type doping), without hydrogen dilution. The substrate temperature was 200 °C and the gas pressure was 600 μbar, leading to a deposition speed of 15–20 Å/s and film thicknesses in the range of 300–500 nm. Nickel was deposited on top of the films by dc sputtering. The Ni concentration was determined on test samples by atomic absorption spectroscopy [15], and varied between 1.6×10^{15} and 1.6×10^{16} atoms/cm^2. Samples were annealed in a furnace at atmospheric pressure under nitrogen flow. After a dehydrogenation step at 400 °C for 24 h, samples were annealed for different periods at temperatures between 500 and 650 °C. Crystallization was controlled through optical microscopy, scanning electron microscopy (SEM), reflectance in the UV and X-ray diffraction.

3. Results and discussion

Fig. 1 (dots) shows the X-ray diffraction spectrum of an as-deposited intrinsic sample. No diffraction peaks are seen in this pattern, suggesting that the as-deposited film is amorphous. This is further confirmed by UV reflectance measurements, which will be presented later. Fig. 2 shows an image—taken with an optical microscope in the reflection mode—of a partially crystallized intrinsic layer (0.3 μm thick). The sample was covered with 3×10^{15} Ni atoms/cm^2, annealed at 550 °C for 12 h, and etched with a Secco solution to reveal the grain boundaries. In the image, disk-shaped grains—some of them with a diameter of ~25 μm and still growing—can be seen.

Fig. 3 is a SEM image of the same layer, focused on a grain boundary region. Inside the grains, some small pockets of amorphous material (etched away by the Secco solution) can still be appreciated. At the grain-growing front, a network structure of branched crystallites can be seen. The width of the needle-like crystallites is about 100 nm. The primary and secondary arms' directions of the needles have the regular angles of 70° or 110° (the so-called bi-directional needle network structure) [16]. This indicates that the crystal exhibits a preferential ⟨110⟩ orientation with respect to the normal to the film surface. It is known that the first stage of the crystallization process is the diffusion of Ni atoms to form a $NiSi_2$ precipitate, which should reach a critical size for the crystallization to proceed

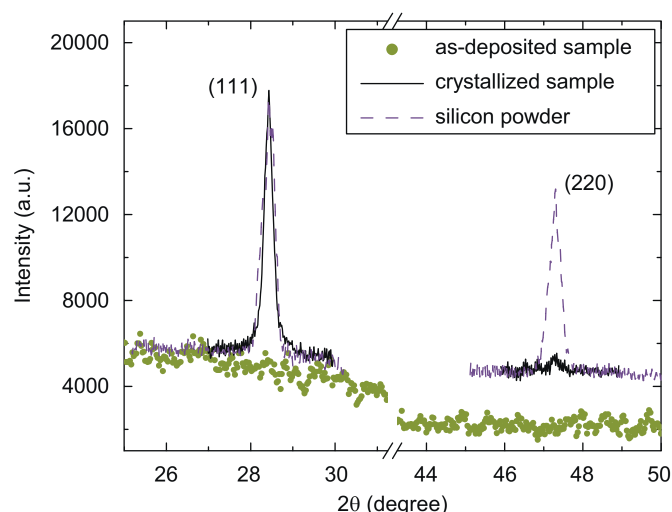

Fig. 1. X-ray diffraction pattern of the intrinsic sample in the as-deposited state (dots) and after annealing at 550 °C for 36 h (solid line). Comparison with the pattern of crystalline silicon powder (dashed line) shows the preferential orientation of the crystallized film.

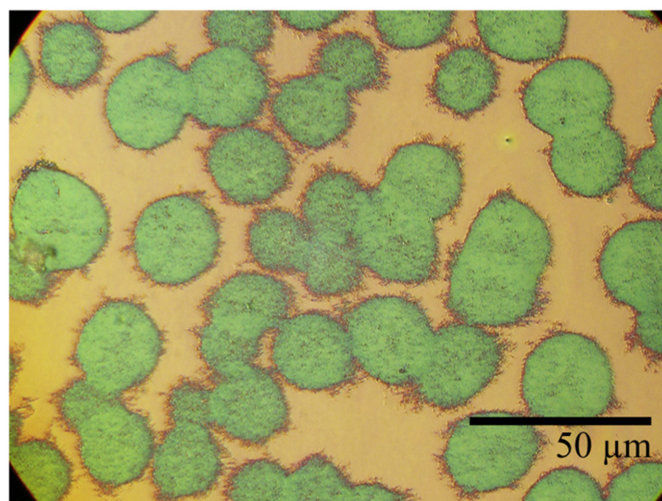

Fig. 2. Reflection optical microscope image of a Secco-etched intrinsic sample annealed at 550 °C for 12 h.

[17]. These $NiSi_2$ precipitates can be formed at as low as 350 °C, in the initial stages of thermal annealing, and act as seeds for the growth of c-Si. $NiSi_2$ forms octahedral precipitates having eight {111} faces. The small lattice mismatch (0.4%) between $NiSi_2$(111) and Si(111) facilitates the formation of epitaxial c-Si on the {111} faces of the precipitates. *In situ* studies revealed that single-crystal Si needles grow in the ⟨111⟩ directions from the migration of $NiSi_2$ precipitates [17,18]. Only ⟨110⟩-oriented $NiSi_2$ precipitates, which have four {111} faces perpendicular to the a-Si surface, can lead to a long-range growth of crystallites. Depending on the thickness of the samples, a mixture of vertical and lateral growth may occur; hence, it is important to study the crystallization of samples having different thicknesses. In the lateral direction the crystalline regions grow until they collide with a neighbor region, so the density of the $NiSi_2$ precipitate determines the grain size. Since the density of the $NiSi_2$ precipitate is related to the average Ni thickness deposited on the a-Si samples, a precise determination of the initial Ni concentration is crucial. Some of the methods employed for this purpose include secondary ion mass spectroscopy, Rutherford

Author's personal copy

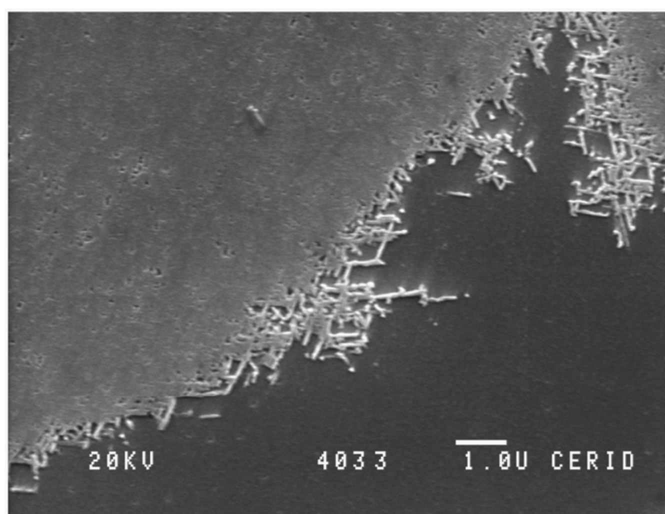

Fig. 3. SEM image of the intrinsic sample of Fig. 2, where a grain boundary region can be seen. The length of the bar is 1 μm.

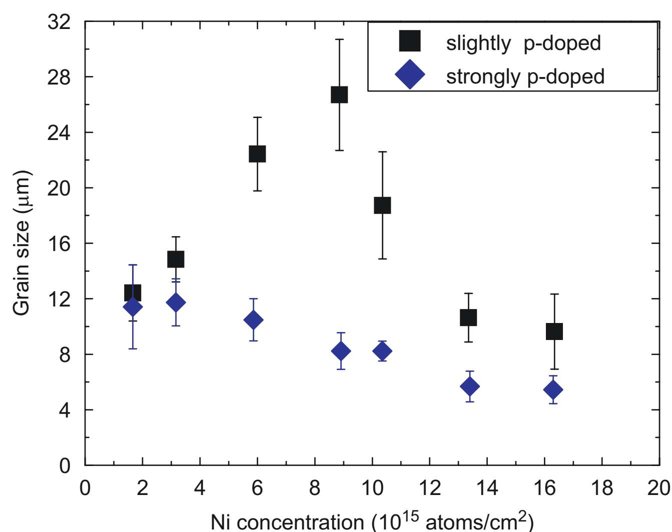

Fig. 4. Average grain size obtained after annealing at 550 °C for 24 h the slightly p-doped (squares) and strongly p-doped (diamond) samples, as a function of Ni concentration.

backscattering spectroscopy, X-ray photoelectron spectroscopy, Auger electron spectroscopy and spectroscopic ellipsometry (SE). The technique employed in this work, atomic absorption spectroscopy [15], is a well-established analytical technique that has sensitivity in the range of parts per billion and can be easily implemented. The remaining Ni concentration in the crystallized samples is also an important parameter for some applications, since the Ni contamination can alter the material properties. SE can also be used to determine the Ni concentration inside the crystallized films, as shown recently [11,19]. In Ref. [11] the authors show that films crystallized from undoped a-Si keep their intrinsic nature, i.e., the Fermi level is located close to the mid-gap of crystalline undoped silicon. This is an indication that at least Ni does not act as an electrically active impurity. Based on this evidence, we do not expect an appreciable effect of Ni contamination on the properties of our samples, since we are using Ni concentrations slightly lower than those reported in Ref. [11].

The preferential orientation of our films is confirmed from the X-ray diffraction spectrum shown in Fig. 1 (solid line), taken for an intrinsic sample after 36 h of annealing at 550 °C. According to the American Standard for Testing Materials (ASTM) card no. 27-1402, the relative integrated intensities for the (111) and (220) peaks are 100:55 for a random Si crystal [20]. From Fig. 1 we obtain the relative integrated intensities 100:5 for the (111) and (220) peaks, which means a higher preferential orientation than in previous reports [3,20,21]. The strong orientation of the grains is important for practical applications, since the material properties should be uniform over the dimensions of the device.

The slightly boron-doped layers ($\sim 10^{16}$ B atoms/cm^3) behave similarly as the intrinsic layers, giving homogeneous polycrystalline films. Fig. 4 (squares) presents the average grain size as a function of Ni concentration, for a series of samples that are 0.5 μm thick. A maximum grain size of (26.7 ± 4.0) μm is obtained for a Ni concentration of 8.8×10^{15} Ni atoms/cm^2. A photograph of this sample, after 24 h of annealing at 550 °C, is presented in Fig. 5. It can be seen that the disk-shaped grains have collided, giving straight grain boundaries. The high crystallinity is confirmed by the UV reflectance measurements as shown in Fig. 6, where the spectrum of this p-doped sample (solid line) is similar to that of a crystalline silicon wafer (dotted line). The small difference may be due to the presence of grain boundaries. Fig. 6 also confirms the amorphous nature of the as-deposited sample (dots). This

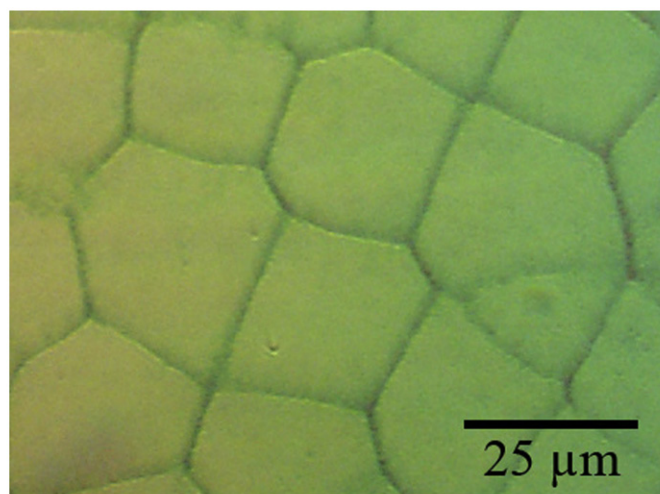

Fig. 5. Reflection optical microscope image of a Secco-etched slightly p-doped sample annealed at 550 °C for 24 h, corresponding to a Ni concentration of 8.8×10^{15} Ni atoms/cm^2.

spectrum, without any distinctive peaks in the UV reflectance, is typical for amorphous silicon.

For higher boron concentrations (as in the p$^+$ samples, $\sim 10^{19}$ B atoms/cm^3), the same sample thickness, Ni concentration and thermal treatment lead to disk-shaped grains of lower diameter, typically <12 μm, as shown in Fig. 4 (diamonds). This may be an indication that boron is promoting the $NiSi_2$ nucleation. In intrinsic a-Si, $NiSi_2$ is usually formed at temperatures above 350 °C. However, in heavily boron-doped Si, Lu et al. [22] reported the formation of $NiSi_2$ at temperatures as low as 250 °C. The substitutional nature of B makes the Ni atoms to behave as more mobile interstitials, thus facilitating the silicide nucleation [14].

Finally, we studied the Ni-induced crystallization of strongly n-doped samples (0.3 μm thick). In this case, we observe that after 12 h of annealing at 550 °C, the nuclei are small and have irregular borders, showing a needle-like crystal growth without a preferential direction (see Fig. 7a). After 36 h of annealing at 550 °C, the crystal grains increase their size without reaching a complete crystallization. To fully crystallize the samples it was necessary to anneal them at 650 °C for 24 h, obtaining a polycrystalline layer

Author's personal copy

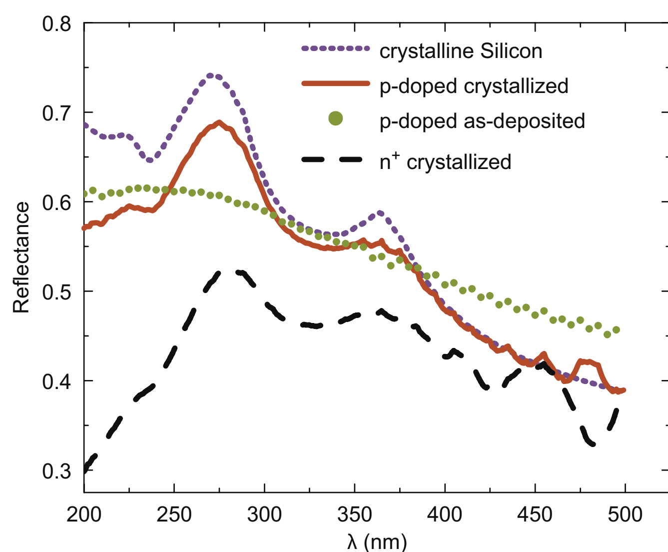

Fig. 6. Reflectance spectra in the UV region of a crystalline silicon wafer, the slightly p-doped sample of Fig. 5, the same slightly p-doped sample in the as-deposited state, and a strongly n-doped sample. The different degrees of crystallization can be observed.

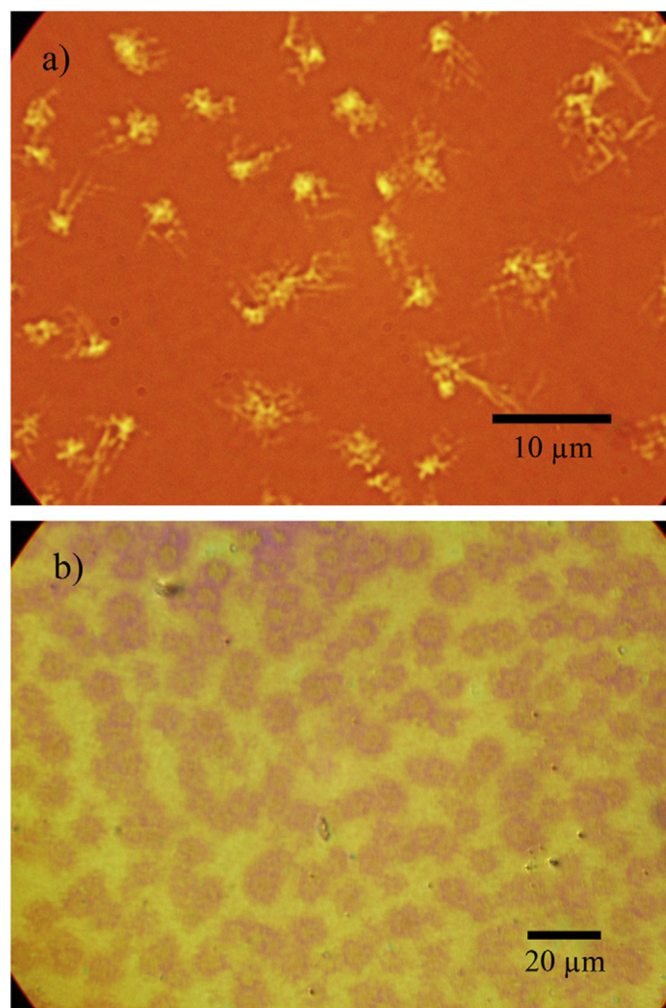

Fig. 7. Optical microscope images of the strongly n-doped sample, after 12 h of annealing at 550 °C (a) and after 24 h of annealing at 650 °C (b).

with a mixture of two types of grains. There are grains of ~7 μm, originated by the $NiSi_2$ nucleus, surrounded by nanocrystals originated in the spontaneous SPC of a-Si at this elevated temperature (Fig. 7b). The mixed nature of the material is also revealed in the UV reflectance spectrum of Fig. 6 (dashed line). This experiment clearly shows that high phosphorous concentrations do not hinder the incubation and nucleation steps, but do strongly affect the growing step. This behavior is in agreement with the results of Ahn et al. [16], who found that the grain growth rate was drastically decreased as the n-type doping increased in their experiments. However, our results differ from reports of Pas et al. [23], who concluded that phosphorous retards the incubation and nucleation steps, and also contradicts reports of Kim et al. [6], who observed that the grains grow into a needle-like shape at low phosphorous concentrations and into a disk-shape at high concentrations. More experiments, including a precise determination of the Ni concentration inside the films, would be needed to clarify the effect of phosphorous doping on silicon crystallization.

4. Conclusion

In summary, we can conclude that the addition of Ni to intrinsic or slightly p-doped a-Si:H layers induces its crystallization with disk-shaped grains larger than 25 μm. This is obtained even on layers of intermediate thickness (0.3–0.5 μm), adding some new information to previous results obtained mostly on thin samples (<0.1 μm). The grains are strongly (111) oriented, which is important for device applications. The presence of large concentrations of dopants like boron or phosphorous leads to a reduction in the grain size. Phosphorous seems to retard the growing step of the crystallization process, although more experiments—including a precise determination of the residual Ni contamination inside the samples—should be performed. The process of silicide-mediated crystallization seems to be appropriate to obtain poly-Si as a base material for solar cells.

Acknowledgments

This work was supported by ANPCyT (Projects 22-20267 and 22-25749), CONICET (Project PIP 5246) and UNL (Project CAI+D 28–158).

References

[1] L. Carnel, I. Gordon, D. Van Gestel, Van Nieuwenhuysen, G. Agostinelli, G. Beaucarne, J. Poortmans, Thin Solid Films 511–512 (2006) 21.
[2] D. Angermeier, R. Monna, A. Slaoui, J.C. Muller, J. Crystal Growth 191 (1998) 386.
[3] J.H. Choi, D.Y. Kim, S.S. Kim, S.J. Park, J. Jang, Thin Solid Films 440 (2003) 1.
[4] I. Hong, T.C. Hsu, S.C. Yen, F.S. Lin, M.L. Huang, C.H. Chen, Surf. Sci. 601 (2007) 301.
[5] Z. Jin, G.A. Bhat, M. Yeung, H.S. Kwok, M. Wong, J. Appl. Phys. 84 (1998) 194.
[6] K.H. Kim, A.N. Nathan, J. Jang, J. Non-Cryst. Solids 354 (2008) 2341.
[7] S.I. Muramatsu, Y. Minagawa, F. Oka, T. Sasaki, Y. Yazawa, Sol. Energy Mater. Sol. Cells 74 (2002) 275.
[8] J.P. Lu, K. Van Schuylengergh, J. Ho, Y. Wang, J.B. Boyce, R.A. Street, Appl. Phys. Lett. 80 (2002) 4656.
[9] A.G. Aberle For recent Rev. See:, Thin Solid Films 511–512 (2006) 26;
K.R. Catchpole, M.J. McCann, K.J. Weber, A.W. Blakers, Sol. Energy Mater. Sol. Cells 68 (2001) 173.
[10] R.B. Iverson, R. Reif, J. Appl. Phys. 62 (1987) 1675.
[11] L. Pereira, R.M.S. Martins, N. Schell, E. Fortunato, R. Martins, Thin Solid Films 511–512 (2006) 275;
L. Pereira, R.M.S. Martins, N. Schell, E. Fortunato, R. Martins, Thin Solid Films 516 (2007) 104.
[12] N. Shibata, K. Fukuda, H. Ohtoshi, J. Hanna, S. Oda, I. Shimizu, Jpn. J. Appl. Phys. 26 (1986) L10.

Author's personal copy

[13] S. Zhao, Z. Meng, C. Wu, S. Xiong, M. Wong, H.S. Kwok, J. Mater. Sci.: Mater. Electron. 18 (2007) S117;
B. Zhang, Z. Meng, S. Zhao, M. Wong, H.S. Kwok, IEEE Trans. Electron. Dev. 54 (2007) 1244.
[14] J.D. Hwang, J.Y. Chang, C.Y. Wu, Appl. Surf. Sci. 249 (2005) 65.
[15] M.B. Sperling, B. Welz, Atomic Absorption Spectrometry, Wiley-VCH, Weinheim, 1999.
[16] J.-S. Ahn, Y.-G. Yoon, S.-K. Joo, J. Crystal Growth 290 (2006) 379.
[17] C. Hayzelden, J.L. Batstone, J. Appl. Phys. 73 (1993) 8279.
[18] M. Miyasaka, K. Makihira, T. Asano, E. Polychroniadis, J. Stoemenos, Appl. Phys. Lett. 80 (2002) 944.
[19] L. Pereira, H. Águas, M. Beckers, R.M.S. Martins, E. Fortunato, R. Martins, J. Non-Cryst. Solids 354 (2008) 2319.
[20] S.Y. Yoon, S.J. Park, K.H. Kim, J. Jang, C.O. Kim, J. Appl. Phys. 87 (2000) 609.
[21] W.S. Sohn, J.H. Choi, K.H. Kim, J.H. Oh, S.S. Kim, J. Jang, J. Appl. Phys. 94 (2003) 4326.
[22] S.W. Lu, C.W. Nieh, L.J. Chen, Appl. Phys. Lett. 49 (1986) 1770.
[23] C.S. Pas, S.S. Lau, I. Suni, Thin Solid Films 109 (1983) 263.